JOURNAL OF CATALYSIS 155, 376–382 (1995)

n-Butane Isomerization over Acidic Mordenite

Raymond A. Asuquo, Gabriele Eder-Mirth, and Johannes A. Lercher

University of Twente, Department of Chemical Technology and Christian Doppler Laboratory for Heterogeneous Catalysis, P.O. Box 217, 7500 AE Enschede, The Netherlands

Received December 6, 1994; revised March 16, 1995

Conversion of *n*-butane was studied between 523 K and 623 K over acidic mordenites with SiO_2/Al_2O_3 ratios between 10 and 20. The main products were *iso*-butane, propane, and pentane. The selectivity to olefins, methane, ethane, C_6 paraffins, and aromatics was lower than 4 mol% under all reaction conditions. Isomerization and disproportionation were identified to be the dominating reactions. At 523 K, both reactions are suggested to proceed via dimeric intermediates. Their relative contributions to the total conversion depend on temperature, partial pressure, and the concentration of the acid sites of the catalyst. The highest yield in *iso*-butane was achieved over a catalyst with a low density of acid sites and at low temperature. At higher temperatures, the rate of isomerization decreased in favor of disproportionation and cracking. A mechanistic model for the isomerization is proposed.

INTRODUCTION

n-Butane forms about 7–12 wt% of the C_4 fraction of the products obtained from catalytic crackers and 2–5 wt% of the products obtained from steam crackers in a typical petroleum refinery (1–3). Significant amounts of *n*-butane are also obtained from wet natural gas.

The largest direct use of *n*-butane is as a component for heating fuel. Because this is a rather low value product, a significant incentive exists to convert *n*-butane to more valuable products. Isomerization of *n*-butane to *iso*-butane is currently important for, e.g., alkylation and production of *iso*-butene for the synthesis of methyl tertiary butyl ether (MTBE), tertiary butyl alcohol (TBA), isoprene, polyisobutene (PIB), and polyisobutene rubber (e.g., (4)).

Commercial processes prior to 1956 employed anhydrous aluminium chloride as the catalyst. Later, a combination of acidic cracking and hydrogenation catalysts such as nickel–silica–alumina, platinum/silica–alumina, or comparable catalysts containing precious metals, as well as organic chlorides, have been used (e.g., (5, 6)). Over these catalysts, the reaction is thought to proceed via dehydrogenation, isomerization of the olefin, and subsequent hydrogenation of the *iso*-alkene. Processes on this basis were commercialized by, e.g., UOP (3). The use of halogen-containing catalysts (to reach the acid strength necessary for skeletal isomerization) is becoming problematic for environmental reasons. Therefore, strongly acidic molecular sieves like H-mordenite offer an interesting alternative to the conventional isomerization catalysts (7–10). The aim of this study is to describe the catalytic properties of mordenites as catalysts for low temperature conversion of *n*-butane and ways to optimize the yield and selectivity of skeletal isomerization and to determine the effect of acid site density in this reaction.

EXPERIMENTAL

Acidic mordenites with SiO_2/Al_2O_3 ratios of 10, 15, and 20 denoted as HM10, HM15, and HM20 (obtained from the Japanese Catalysis Society (11)), respectively, were used. The samples HM15D and HM20D were prepared from HM15 and HM20 by dealumination with HCl. Dealumination was carried out by stirring the zeolites in a 1 *M* solution of HCl (10 ml/g catalyst) for 30 min at room temperature. After filtration and rinsing, the resultant catalyst was dried in air at 390 K for 2 h. Then, the catalyst was calcined in flowing air for 2 h at 600°C (heating rate 5 K/min). The characteristics of the materials used are summarized in Table 1.

The catalytic tests were performed in a fixed bed tubular quartz reactor with an inner diameter of 5 mm operated in continuous flow mode. Between 150 and 200 mg of catalyst were used for each test. The zeolite was diluted with inert quartz in a ratio of 1 : 1. The catalyst was heated in flowing air at 50 K/min up to 823 K. At this temperature it was held for 1 h, and then it was cooled to reaction temperature in flowing air. *n*-Butane (2 vol%) in He (Linde) was used as reactant gas. The reactor effluent was collected with an automatic sampling valve system, stored in multiloop valves and subsequently analyzed by a gas chromatograph HP5890 (50 m Al_2O_3/KCl capillary column) equipped with a flame ionization detector and coupled to a mass selective detector HP 5971A. Coke deposits were determined by temperature programmed

0021-9517/95 $12.00

TABLE 1

Characteristics of the Mordenites Used

	SiO_2/Al_2O_3 bulk	Strong Brönsted acid sites[a]	Extra lattice Al (%)[b]	BET surface area [m^2/g]	Pore volume [cm^3/g]
HM10	10	1.3	8	122	0.07
HM15	15	1.5	11	345	0.15
HM15D	~17[c]	—	15	391	0.18
HM20	20	1.1	>2	388	0.21
HM20D	~25[c]	—	13	336	0.16

[a] Taken from Ref. (11), in [mmol/g].
[b] Determined from ^{27}Al NMR spectra.
[c] Determined from ^{29}Si NMR spectra.

oxidation of the samples on a PL STA 625 V4.30 apparatus. The weight of the coke was calculated as the weight loss between 393 K and 873 K. BET surface area and pore volume were measured on Accelerated Surface Area and Porosimetry (ASAP 2400) equipment.

In order to compare the activities and selectivities of the various catalysts studied, the problem of the fast rate of catalyst deactivation has to be taken into account. Deactivation is caused most probably by acid site poisoning and pore blockage by large polymeric molecules and makes the comparison of the intrinsic activities of the catalysts difficult. Thus, we chose the activities and the rates of decay at a fixed initial and final time on stream (from 30 min to 5 h) for screening of different catalysts under the same experimental conditions.

RESULTS

Effect of the Silica to Alumina Ratio

The activities of the H-mordenite samples (HM10, HM15, and HM20) and their HCl leached derivatives (HM15D and HM20D) as a function of time on stream are shown in Fig. 1. Sample HM15D had the highest

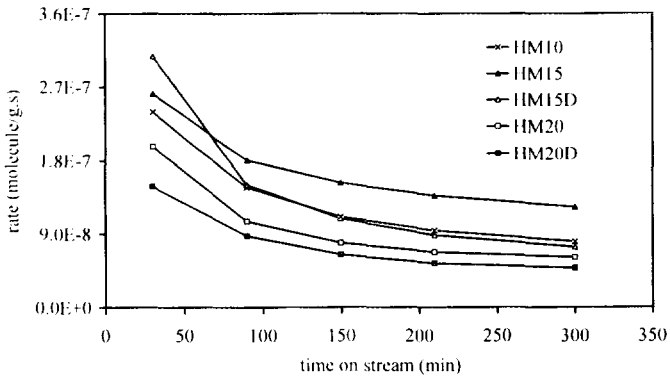

FIG. 1. Rate of *n*-butane conversion over mordenites as function of time on stream. T = 523 K, $p_{p\text{-butane}}$ = 80 mbar, space velocity = 1.12 ml/g s.

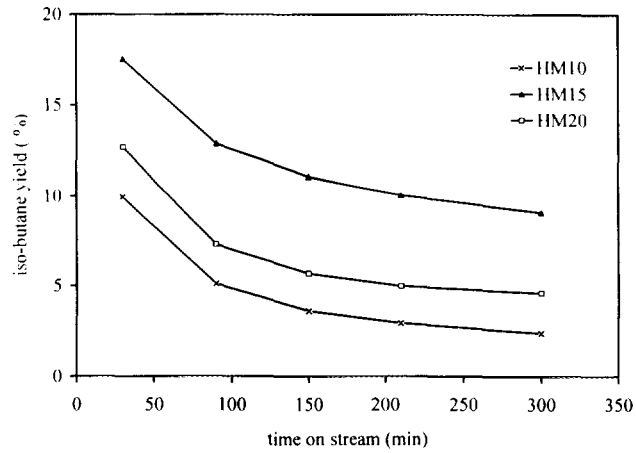

FIG. 2. Yield of *iso*-butane over mordenites as a function of time on stream. T = 523 K, $p_{p\text{-butane}}$ = 80 mbar, space velocity = 1.12 ml/g s.

initial activity, but deactivated more rapidly than the other samples. After 5 h on stream, only 23% of its initial activity was maintained. In contrast, the parent HM15 proved to be the most stable material, having 46% of its initial activity left after 5 h on stream. With HM10 and HM20 (which showed lower initial activities) only 34 and 31% of their initial activities were left after 5 h on stream, respectively.

Figure 2 shows the yield of *iso*-butane for the three parent mordenite samples as a function of time on stream. Disproportionation (formation of propane + pentanes) is the main reaction over HM10, while isomerization is the dominant reaction over HM15, HM20, and their dealuminated derivatives. The ratio of the rates of isomerization to disproportionation as a function of conversion is shown in Fig. 3. Samples with low concentration of acid sites had high initial isomerization activity which continuously

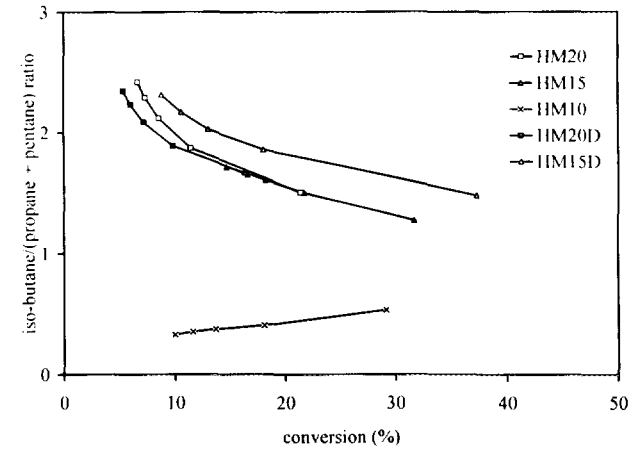

FIG. 3. *Iso*-butane/(propane + pentane) ratio versus conversion over mordenites.

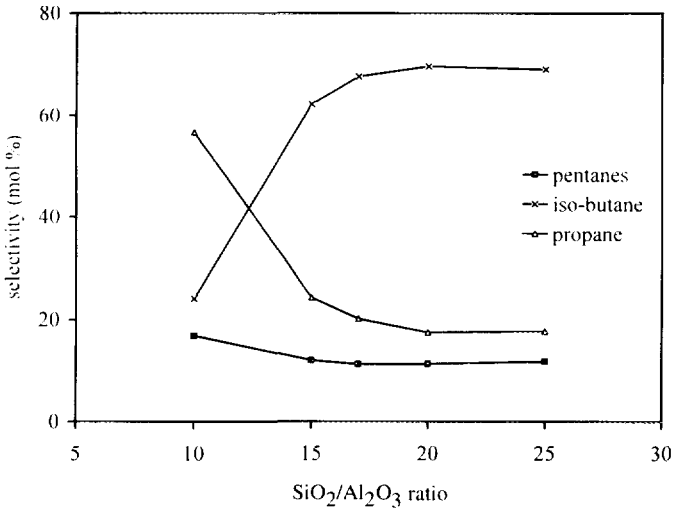

FIG. 4. Product selectivity for *n*-butane conversion versus SiO_2/Al_2O_3 ratio of mordenites after 5 h on stream. T = 523 K, conversion = 10% (HM10), 15% (HM15), 9% (HM15D), 7% (HM20), and 5% (HM20D), $p_{n\text{-butane}}$ = 80 mbar, space velocity = 1.12 ml/g s.

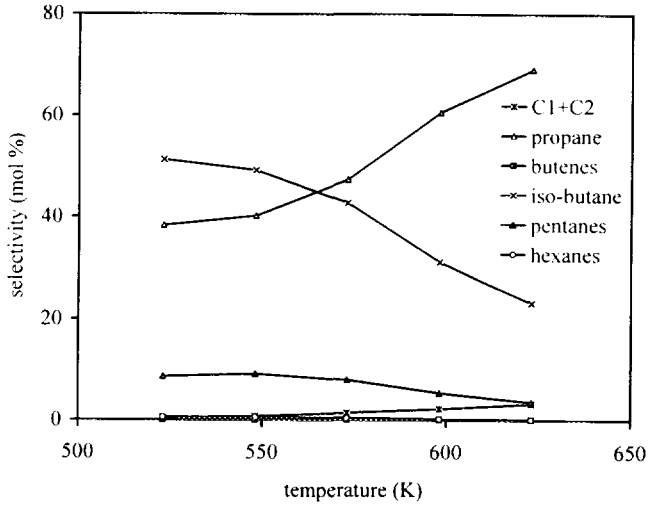

FIG. 6. Product selectivity for *n*-butane conversion as function of temperature over HM20. $p_{n\text{-butane}}$ = 80 mbar, space velocity = 0.88 ml/g s, conversion = 48–75%.

decreased with increasing conversion. On the other hand, the sample with a high concentration of acid sites had low isomerization activity which increased with conversion. After 5 h on stream (Fig. 4), the selectivity to *iso*-butane is higher over HM20 than over HM15. The selectivity to disproportion sharply increased with aluminium content as the reaction approached a steady state.

The product distribution of the three parent mordenites and their HCl leached derivatives at approximately 18% conversion are shown in Fig. 5. The parent HM15 is more stable than all the other samples with a comparable selectivity to *iso*-butane. All dealuminated samples show a slightly higher selectivity to *iso*-butane than their parent

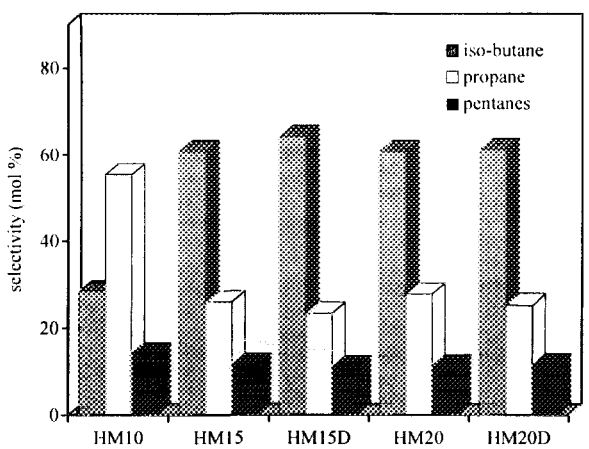

FIG. 5. Product selectivity for *n*-butane conversion over mordenites at approx. 18% conversion. T = 523 K, $p_{n\text{-butane}}$ = 80 mbar, space velocity = 1.12 ml/g s.

analogues. During the reaction (5 h on stream), 3.6, 2.6, and 2.2 wt% of coke was formed on HM10, HM15, and HM20, respectively, which corresponds to 6.6, 3.1, and 4.8 wt% of the converted molecules.

Effect of the Temperature

The product distribution and conversion of *n*-butane over HM20 as a function of temperature (523 K to 623 K) are given in Fig. 6. The selectivity to *iso*-butane decreased (above 560 K very rapidly) while the selectivity to propane increased with temperature. At 523 K, the yield of *iso*-butane over HM20 was 24.6% at a conversion of 48%. At 623 K, at the total conversion of 75%, the yield of *iso*-butane decreased to 17.5%.

Effect of the Partial Pressure

Figure 7 shows the effect of the *n*-butane partial pressure on the rate of *n*-butane conversion over HM20 at three temperatures (523 K, 573 K, and 623 K). The total rate of conversion increased faster with increasing partial pressure at lower temperatures. An apparent kinetic order of 1.5, 1, and 0.5 was determined for the total conversion at 523 K, 573 K, and 623 K, respectively. The effect of *n*-butane partial pressure on the rate of isomerization at the various temperatures is represented in Fig. 8. The apparent kinetic order with respect to *iso*-butane was 1.25, 0.7, and 0 at 523 K, 573 K, and 623 K, respectively. At 523 K, the yield in *iso*-butane changed from 11% ($p_{n\text{-butane}}$ = 40 mbar) to 25% ($p_{n\text{-butane}}$ = 80 mbar); at 573 K, from 15 to 23%; and at 623 K, from 18 to 17% in the same pressure range. The total conversion of *n*-butane increased from 18 to 48%, the yield of propane increased

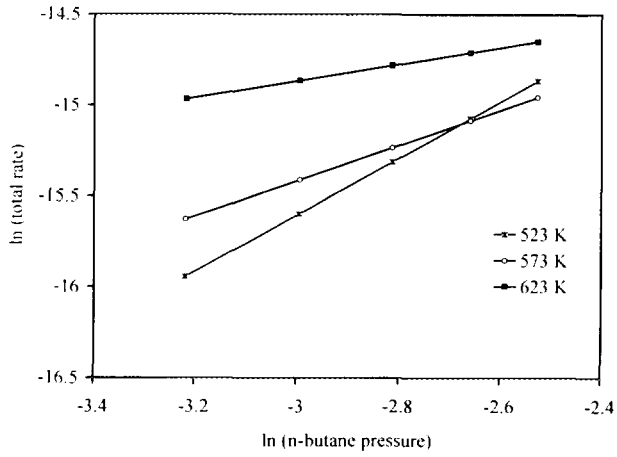

FIG. 7. Effect of *n*-butane partial pressure on the rate of conversion over HM20 at 523 K, 573 K, and 623 K; space velocity = 0.88 ml/g s.

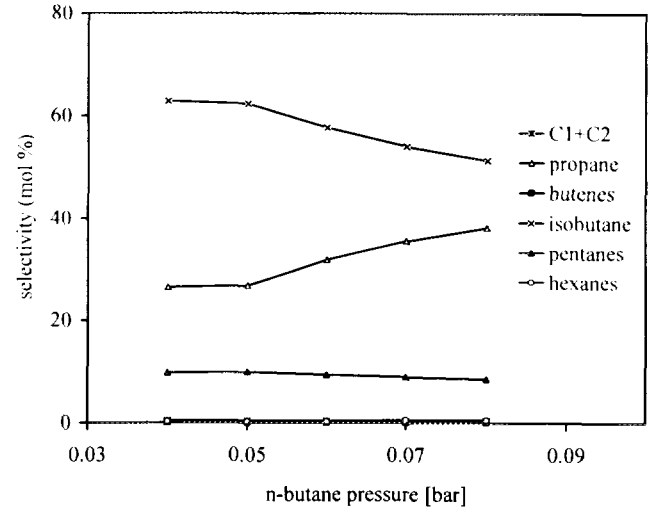

FIG. 9. Effect of *n*-butane partial pressure on the product selectivity of *n*-butane conversion over HM20. T = 523 K, conversion = 18.3–48%, space velocity = 0.88 ml/g s.

from 5 to 18.3% in this pressure interval. The corresponding selectivities at 523 K are shown in Fig. 9.

Effect of the Total Conversion

The product distribution in the *n*-butane reaction over HM20 at low conversions (between 0.5 and 5.3%) is given in Fig. 10. At very low conversion levels, *iso*-butane was the only product. In the yield–conversion plot, *iso*-butane gave a straight line through the origin, indicating that it is a primary product. With increasing conversion, a strong deviation from this behavior was observed, indicating that *i*-butane is also (at higher conversions mainly) formed via a secondary process. The corresponding curves for propane and pentane seem to have zero slope at very low conversions and both products are, thus, concluded to result only from secondary processes.

DISCUSSION

The main products in the conversion of *n*-butane over H-mordenites were *iso*-butane, propane, and pentanes. The selectivity to olefins, methane, ethane, C_6 paraffins, and aromatics was lower than 4 mol% under all reaction conditions. Based on the product distribution obtained and chemical labeling experiments (which indicate extensive scrambling of ^{13}C-marked molecules (12)), we conclude that *n*-butane conversion over H-mordenite at 523 K proceeds predominantly via dimeric or oligomeric

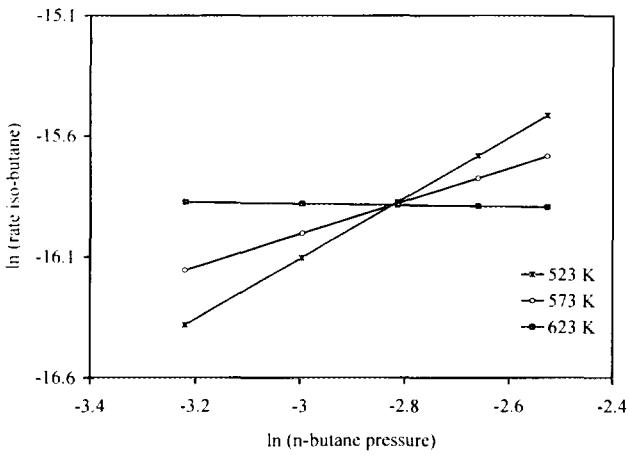

FIG. 8. Effect of *n*-butane partial pressure on the rate of *iso*-butane formation over HM20 at 523 K, 573 K, and 623 K; space velocity = 0.88 ml/g s.

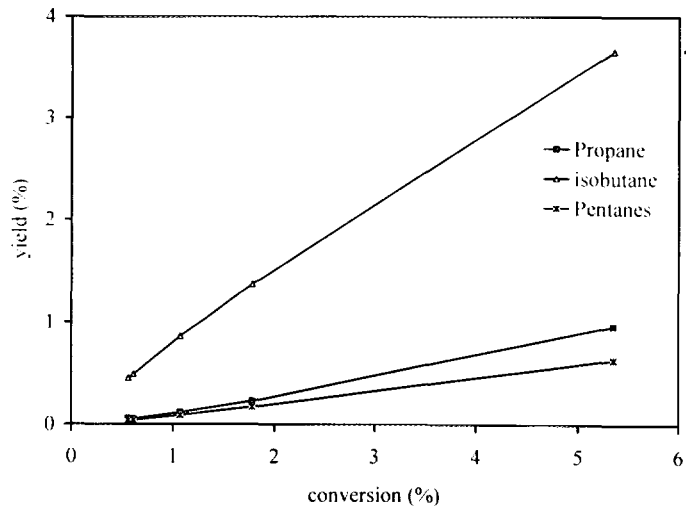

FIG. 10. Yield as a function of *n*-butane conversion over HM20. T = 523 K, $p_{n\text{-butane}}$ = 80 mbar, space velocity = 1–3.5 ml/g s, conversion = 0.5–5.3%.

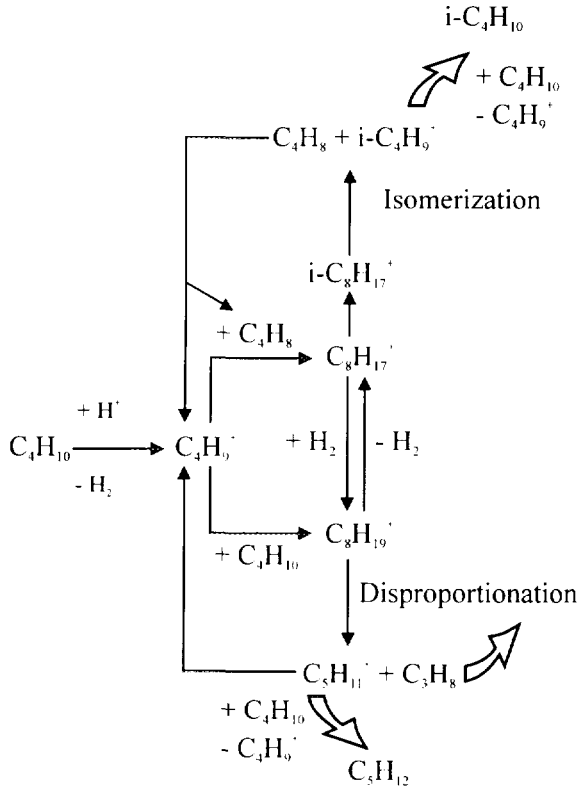

FIG. 11. Reaction scheme of the *n*-butane conversion over mordenites at 523 K.

intermediates (C_8 species), i.e., via a bimolecular pathway.

The dominance of the bimolecular mechanism under the reaction conditions reported here (T = 523 K) can be well explained by the differences in the activation energies of the mono- and bimolecular pathways. Monomolecular isomerization of *n*-butane requires the formation of primary carbenium ions which is reported to proceed at a low rate at temperatures below 570 K. The bimolecular pathway allows us to bypass the formation of primary carbenium ions during the isomerization (e.g., (5, 13, 14)). It has, hence, a lower energy of activation and is generally preferred at low temperatures.

Two main routes of formation and decomposition of the dimeric intermediates might be considered: The first step is in both cases the formation of a butyl carbenium ion via (i) protonation of butane by a surface Bronsted acid site and subsequent abstraction of H_2, (ii) hydride abstraction by a Lewis acid site, or (iii) protonation of trace olefins formed by thermal cracking (15–17). Formally, one can think the dimer to be formed via reaction of the butylcarbenium with an olefin forming a octylcarbenium ion or via reaction with an alkane forming an octyl carbonium ion (5, 18). This can be seen as olefin dimerization and olefin alkylation, respectively (see Fig. 11).

The C_8 carbenium ions formed, mainly 3-methyl C_7 and 3,4-dimethyl C_6, will isomerize readily in the zeolite pores (19) and seem to form preferentially isomers with the methyl group at the C_2 position. These carbenium ions have the positive charge primarily at the tertiary carbon atom and, thus, cracking will yield predominately *n*-butene and *iso*-butene. These molecules will not leave the catalyst without undergoing readsorption and hydrogen transfer with a reactant molecule to form *n*- and *iso*-butane. Thus, *iso*-butane will be the only apparent reaction product.

Cracking of the C_8 carbonium ion is expected to lead to different products. Because propane and pentane are the dominant cracking products, while other hydrocarbons are detected only in minor concentrations, we conclude that a rather specific configuration of the C_8^+ carbonium ion predominates. In the absence of branching, the probability of forming a carbonium ion with the charge at the two central carbon atoms is expected to be very high (20). The saturated molecules resulting from cracking of the adjacent carbon–carbon bonds (α-cracking (e.g. (21))) will then be propane, *n*-butane, and pentane. The remaining carbenium ions (most probably pentylcarbenium ions, as they are expected to be the most stable ones) will leave the surface as saturated hydrocarbons after undergoing hydride transfer with a *n*-butane molecule.

If the carbonium ion is branched, the positive charge is expected to be preferentially located at the tertiary carbon atom. Upon cracking, this would lead to propane and pentene or methane and heptene (which are not observed in resonable concentrations). Again, the alkenes are expected to undergo hydrogen transfer with *n*-butane and leave the zeolite as alkanes.

However, irrespective of the route of formation of the C_8 species, the relative concentrations of carbenium and carbonium ions will depend to a large extent upon the hydrogen transfer ability of the zeolite. If we agree that the ratio of the rates of isomerization to disproportionation reflects the concentration of carbenium and carbonium ions on the catalysts, it is primarily the ability for hydrogen transfer, which determines the selectivity of the mordenite catalysts.

It is interesting to see how selectivity changes with the chemical composition of the zeolite. We choose the *iso*-butane/(propane + pentane) ratio as measure for the isomerization versus disproportionation activity of the catalyst. A low value (as found with HM10) indicates high disproportionation activity (related to high hydrogen transfer), while a high value (as found with HM20) suggests high isomerization and lower hydrogen transfer activity. As shown in Fig. 4, the selectivity to *i*-butane decreased in the sequence HM20 > HM15 > HM10, i.e., with decreasing acid site concentration on the catalyst.

These findings are in good agreement with the fact that zeolites with high concentrations of Bronsted acid sites possess a high hydrogen transfer activity which leads to a shorter lifetime of carbenium ions in the zeolite pores. Consequently, octylcarbenium ions sorbed on zeolites with a low concentration of acid sites have a longer lifetime and can, thus, undergo secondary reactions like isomerization several times before being cracked (22).

To verify the mechanism outlined above, Krupina *et al.* (10) studied the transformation of potential intermediates (*n*-octane and *iso*-octane) under comparable conditions. The product distribution was identical to that of *n*-butane conversion over H-mordenite. Note that dimeric molecules in *n*-butane conversion were also proposed to occur over solid superacids like $Al_2O_3/AlCl_3$ (5). Thus, it was speculated that similarities exist between the catalytic properties of H-mordenites and those of liquid superacids (23).

The low selectivity in *iso*-butane obtained with HM10 in this study agrees also well with the results of Corma *et al.* (20, 22) on *iso*-butane/2-butane alkylation over ultra stable zeolite Y. The authors proposed two competing reactions pathways for the formation of the C_8 hydrocarbons, the direct addition of *i*-butane to adsorbed 2-butene (alkylation route) and the dimerization reaction of two olefine molecules (oligomerization route) (22). The alkylation/oligomerization ratio increased with increasing Al concentration in the zeolite. This was explained by the need of high concentrations of reactants in the zeolite pores in order to obtain high alkylation activity. In the present study, the highest disproportionation (corresponds to high alkylation) selectivity in the *n*-butane conversion was found with HM10, the sample with the highest Al concentration. While the catalysts with low concentrations of acid sites (HM15, HM20, and their dealuminated analogues) were preferentially active for isomerization (corresponds to oligomerization). Note that the selectivity to *iso*-butane is lowered upon increasing the partial pressure of the reactant (i.e., favored reaction conditions for alkylation) at 523 K (compare Fig. 9).

Alternatively, however, it could also be argued that high concentrations of strong Brönsted acid sites provide sufficient sorption sites for butenes (formed by protolytic dehydrogenation) so that reactions between butanes and butenes might dominate (disproportionation route). In contrast, zeolites having low concentrations of strong Bronsted acid sites will sorb only a fraction of the butenes formed, facilitating the less demanding butene oligomerization (isomerization route). The lower selectivity toward *iso*-butane with increasing reaction temperature (which also leads to a lower concentration of sorbed molecules at constant partial pressure) appears to be inconsistent with the above arguments. However, the energies of activation for cracking via the carbonium ion route are higher than those for the carbenium ion route and, thus, the former reaction will gain sharply in importance with increasing reaction temperature. At high conversions, the lower thermodynamic equilibrium concentrations of *iso*-butane with increasing reaction temperature might also lower the selectivity.

The reaction rate varied in parallel to the concentration of strong Bronsted acid sites as determined by Sawa *et al.* (11; the values are included in Table 1) for the present samples. This indicates that only the strongest acid sites (i.e., the hydroxyl groups at isolated tetrahedral Al in the lattice) contribute to the catalytic action of the zeolites studied (24, 25).

In this respect it is also important to mention that the pentane isomers were always near to their thermodynamic equilibrium concentrations over HM15, HM20, and their dealuminated analogues. This was not the case with HM10 and is attributed to a slower rate of skeletal isomerization over this catalyst leading to the preferential formation of *n*-pentane. It seems likely that the *iso*-pentyl-carbenium ions preferentially dehydrogenate to give coke precursors. Alternatively, these carbenium ions are speculated to first oligomerize and then undergo consecutive cracking, resulting in an increase in the concentration of propane in the product stream and a higher rate of coke formation. We would like to speculate that such reactions cause the propane/pentane ratio to exceed the theoretical value of 1 even at low conversion levels.

CONCLUSION

Over H-mordenites, *n*-butane is mainly converted via a bimolecular mechanisms at low temperatures. Hydrogen transfer is suggested to play a decisive role for the product distribution. Isomerization and disproportionation are the main reactions. The relative importance of the two reaction routes depends subtly upon the reaction temperature, the concentration of acid sites, and the conversion.

In the first step, *n*-butane is suggested to form a butylcarbenium ion by protonation at the strong Bronsted acid sites and subsequent dehydrogenation. With samples of low concentration of Bronsted acid sites the butylcarbenium ion is concluded to predominantly react with a butene molecule to form a sorbed octylcarbenium ion which subsequently isomerizes. The branched C_8^+ species cleaves by forming *iso*-butene and *n*-butene. The formed alkenes are readsorbed prior to leaving the zeolite and undergo hydride transfer with a reactant molecule to form alkane molecules or a carbenium ion which stays adsorbed at the catalyst. This carbenium ion takes part again in the reaction cycle, leaving *iso*-butane as the only apparent reaction product (isomerization route).

If the concentration of acid sites exceeds a certain value (i) alkylation of the sorbed butylcarbenium ion by a butane

molecule and/or (ii) hydride transfer to a octyl carbenium ion resulting in an octyl carbonium ion become the dominating reactions. As the charge in a carbonium ion is preferentially located on the inner carbons, this carbocation cracks mainly into propane and a pentylcarbenium ion which leaves the catalyst as pentane after hydride transfer with a *n*-butane molecule (disproportionation route).

At higher reaction temperatures and higher conversions, part of the *iso*-butane formed is suggested to again take part in the reaction cycle. That means, it will react with a carbenium ion by forming a C_8^+ intermediate, which will finally crack into C_3 and C_5 alkanes, leading to an increase in the selectivity toward disproportionation.

There is strong evidence that high concentrations of molecules in the zeolite pores (favored by a high site density and high partial pressures) direct the conversion of *n*-butane toward disproportionation. Thus, it is mandatory for a successful *n*-butane isomerization catalyst to have a low concentration of strong Bronsted acid sites. The process conditions should be chosen in a way to avoid too high concentrations of alkanes in the zeolite pores. The reaction has to be carried out at low temperatures, not only because of the thermodynamic limitations to form *iso*-butane, but also because at higher reaction temperatures the higher energy of activation makes the disproportionation pathway the preferred reaction route.

ACKNOWLEDGMENT

We gratefully acknowledge the financial support of the Christian Doppler Laboratory.

REFERENCES

1. Ashworth, M. R. F., in "C_4-Hydrocarbons and Derivatives." Springer-Verlag, Berlin, 1989.
2. Sie, S. T. *Stud. Surf. Sci. Catal.* **85,** 587 (1994).
3. Maxwell, I. E., and Stork, W. H. J., *Stud. Surf. Sci. Catal.* **58,** 571 (1991).
4. Vesely, V., and Mostecky, J., *in* "Petrochemia," 221. 1989.
5. M. Marcewski, *J. Chem. Soc. Farad. Trans. I* **82,** 1687 (1986).
6. Sie, S. T., *Stud. Surf. Sci. Catal.* **85,** 620 (1994).
7. Kouwenhoven, H. W., and van Zijll-Langhout, *Chem. Eng. Process.* **67,** 65 (1971).
8. Moulijn, J. A., Sheldon, R. A., van Bekkum, H. and van Leeuwen, *in* "Catalysis." p. 33. Elsevier, Amsterdam, 1993.
9. Bearez, C., Chevalier, F., and Guisnet M., *React. Kinet. Catal. Lett.* **22**(3–4), 405 (1983).
10. Krupina, N. N., Proskurin, A. L., and Dorogochinski, A. Z., *React. Kinet. Catal. Lett.* **32**(1), 135 (1986).
11. Sawa, M., Niwa, M., and Murakami, Y., *Zeolites* **10,** 532 (1990).
12. Bearez, C., Avendano, F., Chevalier, F., and Guisnet, M., *Bull. Soc. Chim.* 346 (1985).
13. Chevalier, F., Guisnet, M. and Maruel, R., Proc. 6th ICC, London, 478 (1977).
14. Mooiweer, H. H. deJong, K. P., Kaushaar-Czarnetzki, B., Stork, W. H. J., and Krutzen, B. C. H., *Stud. Surf. Sci. Catal.* **84,** 2327 (1994).
15. Haag, W. O. and Dessau, R. M., Proceedings, 8th International Congress on Catalysis, Berlin, 1984. Dechema, Frankfurt-am-Main, 1984.
16. Shigeishi, R., Garforth, A., Harris, I., and Dwyer, J., *J. Catal.* **130,** 423 (1991).
17. Guisnet, M., Gnep, N. S., Aittaleb, D., and Doyemet, Y. J., *Appl. Catal. A* **87,** 255 (1992).
18. Olah, G. A., Halpern, Y., Shen, J., and Mo, Y. K., *J. Am. Chem. Soc.* **95**(15), 4960 (1973).
19. Wojciechowski, B. W., and Corma, A., in "Catalytic Cracking," p. 32. Dekker, New York, 1986.
20. Narbenshuber, T., Doctoral thesis, University of Twente, The Netherlands, 1994.
21. Krannila, H., Haag, W. O., and Gates, B. C., *J. Catal.* **135,** 15 (1992).
22. Corma, A., Martinez, A. and Martinez, C., *J. Catal.* **146,** 185 (1994).
23. Albright, L. F., *Oil Gas J.* 79 (1990).
24. Guisnet, M., Fouche, V., Bellum, M., Bournonville, J. P., and Travers, C., *Appl. Catal.* **71,** 283, 295 (1991).
25. Koradia, P. B., Kiovski, J. R., and Asim, M. Y., *J. Catal.* **66,** 290 (1980).